Assessment of the Possibility of Natural Spread of Citrus Psorosis Disease in Texas

T. R. Gottwald[1], S. R. Palle[2], H. Miao[2], M. Seyran[2], M. Skaria[2], and J. V. da Graça[2]

[1]USDA-ARS USHRL, 2001 S. Rock Road, Ft. Pierce, FL 34945, USA;
[2]Texas A & M University-Kingsville Citrus Center, Weslaco, TX 78596, USA

ABSTRACT. Observations in Argentina, Texas and California several years ago on the increase in incidence of citrus psorosis symptoms in the field suggested a possible natural spread of the disease. Specifically, past and more recent observations on the incidence of psorosis in Texas in nucellar Redblush grapefruit trees and in originally virus-free Rio Red grapefruit trees also support the hypothesis that natural transmission occurs. The incidence of psorosis symptoms in four orchards of grapefruit trees was recorded annually over a 3-yr period, rating trees on a scale of 0 (no symptoms), 1 (some bark peeling and/or gumming), 2 (psorosis-like scaling) and 3 (classic psorosis bark-scaling). To assess the possibility of biotic cause of psorosis spread, the spatial arrangement of infected plants was examined at different spatial scales (single tree, groups of plants, and whole plantings) and stochastic simulation models were used to predict the likelihood and contribution of potential exogenous versus endogenous sources of inoculum. Aggregation was observed both at the single tree, and groups scale that decreased through time. Some evidence of relationships among groups of diseased trees was also observed and stochastic models indicated the likelihood of background (exogenous) sources of inoculum. These spatial and spatio-temporal findings are consistent with expected disease spread via vectors although two different possible cases of spread could be identified among the four plots. *Citrus psorosis virus* is the type member of the *Ophiovirus* genus, and there is evidence that other members are transmitted through the soil by *Olpidium brassicae*.

The high incidence of citrus psorosis disease in Texas in the 1940s (3) led to the launching of a budwood certification program in 1948 (21). Although many psorosis-free trees were propagated, the program was voluntary and ceased to exist by 1959. However, the use of virus-free budwood sources, and the effects of four tree-killing freezes between 1951 and 1989 are believed to have been responsible for a dramatic reduction in the disease (19). Timmer and Garnsey (22) observed that trees that were of nucellar origin were showing bark scaling symptoms of psorosis, and suggested that a vector may be involved (22). Research in Argentina also provided evidence that psorosis appears to spread naturally in the field (1). More recently, observations again in Texas have suggested natural spread of this disease (18, 20). The characterization of *Citrus psorosis virus* (CPsV) as the type member of the genus *Ophiovirus* and demonstration of transmission of another ophiovirus in lettuce by the fungus *Olpidium brassicae* (11), initiated a study on the possibility of transmission of CPsV by a root-infecting fungus. It should be noted that not all bark-scaling symptoms in citrus are associated with CPsV; this has been found in Spain (16), as well as in Brazil, French Polynesia and elsewhere (17). In our studies, random samples from trees with typical bark scaling symptoms tested positive for psorosis by biological indexing, ELISA and PCR (18). Orchards with infected trees were mapped to examine the spatial patterns of psorosis symptoms and how these patterns changed through time in an attempt to better understand the underlying mechanisms that contribute to the spread of psorosis.

MATERIALS AND METHODS

Data collection and preparation. The incidence of psorosis symptoms in four grapefruit orchards on

sour orange (A4, B5, E1 and F1) of the Texas A & M University-Kingsville Citrus Center was recorded annually over a 3-yr period (2002-2004). The number of trees surveyed was 713 (A4), 129 (B5), 539 (E1) and 612 (F1), making a total of 1,993. The disease status of each tree was recorded rating trees on a scale of 0 = no symptoms, 1 = some bark peeling and/or gumming, 2 = small areas psorosis-like scaling, and 3 = typical psorosis bark-scaling and some leaf ringspots. Biological indexing of 13 trees with symptoms selected by nonprobabilistic sampling confirmed psorosis disease was present. ELISA (23 positive/24 trees with leaf ringspot symptoms, and 18/27 with bark scaling) and PCR tests (8 positive/9 trees) of selected trees provided further confirmation. All assays were conducted as described elsewhere (18). There was a bit of uncertainty relative to the lowest disease rating of 1, which could be related to the initial phases of psorosis infection or could be related to other non-viral causes. Therefore, for analysis purposes, two scenarios were considered to partition the ratings into two groups. For scenario 1, a rating of 0 or 1 was considered psorosis-free and a rating of 3 or 4 was considered psorosis infected. For scenario 2, a nondiseased situation was attributed to a rating of 0, and all other ratings of 2, 3, or 4 were considered indicative of psorosis infection. Because bark scaling symptoms can take an average of 12 yr to appear (23), it is probable that some symptomless trees in this study were already infected, but it was assumed that infection would have likely occurred after other trees showed symptoms. A 0 rating is therefore either a healthy tree, or an asymptomatic infected tree.

Spatial analysis. Binary (presence/absence) spatial maps of psorosis were prepared for all assessment dates for each plot. For the first level of spatial hierarchy, ordinary runs analyses were performed on each data set to determine if aggregation existed between adjacent symptomatic trees within rows and across rows with the use of a Visual Basic EXCEL macro (14, 15, and Gottwald, unpublished data). A nonrandom pattern (i.e., aggregation) of symptomatic trees was assumed if the observed number of runs was less than the expected number of runs at $P = 0.05$.

For the second level of spatial hierarchy, the data were examined for the presence of aggregation at various quadrat sizes. The incidence data for each plot were partitioned into quadrats of four (2 by 2), trees with the use of a Visual Basic EXCEL macro (Gottwald, unpublished data). When data are expressed as disease incidence, the beta-binomial distribution provides the best fit for random conditions (13). Randomness within quadrats was thus assessed via beta-binomial analysis. The beta-binomial index of dispersion D was used to test for the presence of randomness of symptomatic trees at each quadrat size (10, 13). For the beta-binomial index, a large D (>1) combined with a small P (<0.05) suggests aggregation of symptomatic trees (12).

In the third level of spatial hierarchy, the strength and directionality or orientation of aggregation among quadrats of various sizes containing symptomatic citrus trees for 20 plots were examined with spatial autocorrelation analysis (7). Data were parsed into quadrat of 2×2, trees. The x,y spatial location and disease incidence of trees within each quadrat size on each assessment date in the individual citrus plots were used as input data. Autocorrelation proximity patterns were calculated consisting of positively (SL+), negatively (SL-), and non-correlated lag positions from which an evaluation of spatial patterns of disease incidence was performed. The size and shape of core and reflected clusters of SL+ were calculated, in which a core cluster is a group of significant, positively correlated (P = 0.05), spatial lag distance classes

that form a discrete and contiguous group with the origin (i.e., lag [0.0]) of the autocorrelation proximity pattern; a reflected cluster is a discrete group of two or more contiguous significant positive lag positions discontiguous with the origin and the core cluster. The strength of aggregation is a measure of the saturation of the core clusters with significantly positive lags (i.e., the proportion of lag positions within the extents of the cluster that were significantly positive). Row effects were evaluated as the number of significant lag positions within the first row (within) or within the first column (across) of the autocorrelation proximity pattern that are contiguous with the origin (2, 8, 23).

Spatio-temporal analysis. Data for the psorosis epidemics were analyzed using the spatio-temporal stochastic model for disease spread which was fitted using Markov-Chain Monte Carlo (MCMC) stochastic integration methods. For a thorough description of the MCMC model, its application and interpretation of results, refer to Gibson (4, 5, 6). The results of the spatio-temporal analysis can be viewed graphically in a two-dimensional parameter space representing a series of 'posterior density' contours of parameter densities. The two parameters represent local (a_2) versus background (b) interactions. The parameter b quantifies the rate at which a susceptible individual acquires the disease due to primary infection independent of the infected trees in the plot and is therefore is the simple interest or primary infection rate in a spatio-temporal context. For many viruses and other pathogens that are vector transmitted and dispersed, this usually means from sources of inoculum outside of the host population, i.e., plot. However, for soilborne pathogens, it can also represent an increase in disease due to resident inoculum in the soil as well as from other sources such as outside the plot. Whereas a_2 represents the secondary infection rate in a spatio-temporal context, and quantifies the manner in which the infective challenge presented to a susceptible individual by a diseased individual in the population decreases with the distance between them. As a_2 increases, the secondary transmissions occur over shorter ranges and, so long as b is not so large that primary infections dominate, disease maps generated by the model exhibit aggregation.

RESULTS AND DISCUSSION

All trees recorded as having symptoms in one year, either had the same rating or higher the following years. Fig. 1 shows the increase in the percentage of trees in each of the four blocks with bark scaling (scenario 2) for the 3-yr survey period.

Spatial arrangement of psorosis-symptomatic trees. The first level of spatial hierarchy examined was the association of symptom status between adjacent psorosis infected trees. Only a small percentage of within-row or across-row tests expressed aggregation of psorosis-infected trees in either direc-

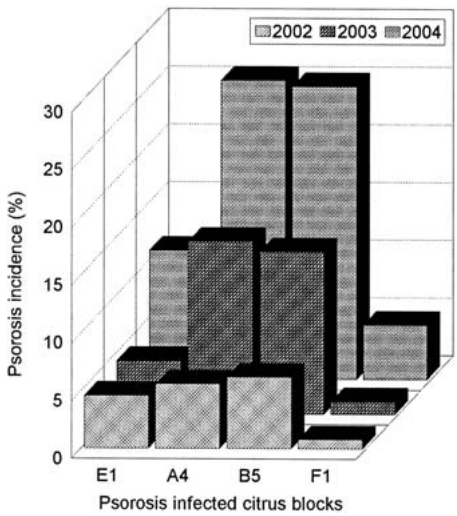

Fig. 1. Percentage of grapefruit trees displaying psorosis bark scaling symptoms in four blocks in south Texas over a 3-yr period.

tion among all of the plot/year combinations of data sets (Table 1). Scenario 2 had a slightly higher proportion of aggregated tests due to the greater disease incidence attributed to this scenario. However, when plots were considered one long line of trees, 41.6 and 58.3% of tests suggested a nonrandom spatial pattern for within- and across-row orientations. Therefore, aggregation was detectable at the individual tree level but was not strong.

The next level of spatial hierarchy to be examined was the association of symptomatic plants within quadrats (groups of 2×2 plants). The interpretation of the values of the beta-binomial index of dispersion (D) suggests a spatial structure of symptomatic plants significantly nonrandom for 4 of 9, and 3 of 10 plot/year combinations tested for scenario 1 and scenario 2, respectively, for which the beta-binomial test could be conducted (Table 2). For 33% of the plot/year combinations for both scenarios tested, D values were higher than 1, i.e., aggregated but did not seem to be related to disease incidence. Therefore, aggregation was detectable at the group level also, but like the individual tree level, it was not strong.

The final level of spatial hierarchy examined was the association among groups (quadrats) of trees as estimated by spatial autocorrelation. For the 2×2 quadrat size, small core clusters consisting of only a single adjacent group, were found in seven of 24 tests and core clusters with more than a single adjacent group of psorosis

TABLE 1
ORDINARY RUNS ANALYSIS OF PSOROSIS IN FOUR CITRUS BLOCKS IN SOUTH TEXAS

Plot	Year	Scenario	Disease incidence	Ordinary runs			
				Row	Column	Row (all)	Col (all)
A-4	2002	Scenario 1	0.156338	0/30	1/21	R	N
		Scenario 2	0.5	3/34	1/21	N	R
	2003	Scenario 1	0.232117	1/33	4/21	N	N
		Scenario 2	0.550365	1/33	2/21	R	N
	2004	Scenario 1	0.262774	1/33	5/21	N	N
		Scenario 2	0.626277	1/33	3/21	R	N
B-5	2002	Scenario 1	0.129496	0/12	1/7	R	R
		Scenario 2	0.438849	0/19	1/8	N	N
	2003	Scenario 1	0.235294	0/17	0/8	R	R
		Scenario 2	0.602941	0/20	1/8	N	N
	2004	Scenario 1	0.235294	0/17	0/8	R	R
		Scenario 2	0.647059	0/19	2/8	N	N
E-1	2002	Scenario 1	0.0909091	0/30	1/9	N	N
		Scenario 2	0.307978	4/53	3/10	N	N
	2003	Scenario 1	0.103896	0/32	1/10	N	N
		Scenario 2	0.376623	4/55	1/10	R	R
	2004	Scenario 1	0.111317	0/33	2/10	N	N
		Scenario 2	0.395176	3/55	3/10	R	N
F-1	2002	Scenario 1	0.0359477	0/16	0/10	R	R
		Scenario 2	0.333333	3/48	2/13	R	R
	2003	Scenario 1	0.0473856	0/19	0/9	R	R
		Scenario 2	0.343137	3/48	2/13	R	R
	2004	Scenario 1	0.0473856	0/19	0/9	R	R
		Scenario 2	0.370915	3/48	3/13	R	N

Values shown for each plot in each assessment date are the proportion of the number of test rows with significant aggregation ($P = 0.05$) divided by the total number of rows tested (row with more than 1 diseased tree).
Row (all) and Col (all) tests consider the plot as one long row or column respectively. R = random or non aggregated situation indicated. N = non-random or aggregated situation indicated.

TABLE 2
BETA-BINOMIAL PARAMETER AND DISPERSION INDEX FOR PSOROSIS INCIDENCE IN FOUR CITRUS BLOCKS IN SOUTH TEXAS

Plot	Year	Scenario	Disease incidence *p*	Beta-binomial parameter (?)	Dispersion Index (*D*)[b]
				Quadrat 2 × 2[a]	Quadrat 2 × 2
A-4	2002	1	0.156338	0.0735507*	1.21186*
		2	0.5	0.0795065*	1.22791**
	2003	1	0.232117	0.0488198	1.14063
		2	0.550365	0.045583	1.14025
	2004	1	0.262774	0.0201918	1.06869
		2	0.626277	0.029585	1.10199
B-5	2002	1	0.129496	0.0957519	1.18322
		2	0.438849	0.213857	1.46639*
	2003	1	0.235294	0.12417	1.31036
		2	0.602941	0.277041*	1.54741**
	2004	1	0.235294	0.12417	1.31036
		2	0.647059	0.352268*	1.66835***
E-1	2002	1	0.0909091	0.131118*	1.3249**
		2	0.307978	0.0168484	1.06593
	2003	1	0.103896	0.1047*	1.29181*
		2	0.376623	0.0138735	1.0532
	2004	1	0.111317	0.113808*	1.30008**
		2	0.395176	0.0444073	1.13467
F-1	2002	1	0.0359477	0	0.880011
		2	0.333333	0	0.924655
	2003	1	0.0473856	0	0.839172
		2	0.343137	0	0.970032
	2004	1	0.0473856	0	0.839172
		2	0.370915	0.0548352	1.17827

[a]Maximum likelihood estimate of the beta-binomial aggregation parameter θ. Significant departures from zero were determined by a t test, t = θ/s.e.(θ)) and indicated overdispersion. Significance is indicated by *, **, *** at respectively $P = 0.05$, $P = 0.01$ and $P = 0.001$. Values in italic indicate that the likelihood estimation procedure of the p and θ parameters of the beta binomial distribution has failed and that the parameter θ was calculated using the moment method but its departure from zero could not be tested (24).

[b]Index of dispersion (*D*) values for the indicated quadrat size by plot and assessment date for psorosis infected citrus plots in south Texas. Values presented for each assessment date are *D* (=observed variance/binomial variance). Tests for aggregation were performed by comparison of (N-1)x *D* with the chi-square distribution and with the C(α) test (Z statistic) as described in the text. Significance *,**,*** is indicated for the C(α) test. A large (>1) *D* and a small *P* (≤0.05) suggest rejection of H_0 (binomial distribution- random pattern of symptomatic trees) in favor of H_1 (overdispersion described by the beta-binomial).

positive trees were found in only two of 24 tests (plot A-4 in 2003 and for E1 in 2004). When core clusters larger that one adjacent lag were indicated, they were incompletely saturated, meaning that they were in loose groups rather than complete compact groups with no missing infected trees (Table 3). There did not seem to be a greater prevalence related to one scenario versus another. Reflected clusters of psorosis-positive trees were found in 9 of 24 plot/year/scenario combinations but were small in size and not prevalent. Where these reflected clusters did exist, they ranged from 13.2 to 51.8 m from the centroid of the main cluster (Table 3).

There was a slightly greater number of aggregations in the within-row direction than the across-row direction and very few edge effects. Thus aggregation was again present but not particularly strong among groups of trees, but there was some evidence of longer distance associations among groups of trees. There also did not appear to

TABLE 3
SPATIAL AUTOCORRELATION ANALYSIS OF FOUR PSOROSIS-AFFECTED CITRUS BLOCKS IN SOUTH TEXAS

Plot	Year	Scenario	Disease incidence[a]	Significant lags[b]		Strength of aggregation[c]	Core cluster size[d]	Core cluster saturation[e]	Reflected cluster size[f]	Total no. of reflected clusters[g]	SL+ reflected clusters[h]			Effects[i]		
				SL+	SL-						Max. X dist.	Max. Y dist.	Calc dist. (m)	Within row	Across row	Edge
A-4	2002	1	0.464706	1	0	0	0	NA	1	1	0	6	32.9	1	0	0
		2	0.923529	2	0	0	0	NA	1	2	2	6	36.0	1	0	1S
	2003	1	0.6	7	0	0.714286	5	0.555556	2	1	0.5	6	33.1	5	1	0
		2	0.923529	3	0	0.333333	1	1	1	2	6	5	51.8	2	0	0
	2004	1	0.676471	5	2	0.2	1	1	4	1	0	3.5	19.2	4	1	0
		2	0.952941	4	0	0.25	1	1	1	3	6	5	51.8	2	1	0
B-5	2002	1	0.333333	0	0	0	0	0	0	0	NA	NA		0	0	0
		2	0.666667	1	0	1	1	1	0	0	NA	NA		1	0	1S
	2003	1	0.458333	0	0	0	0	0	0	0	NA	NA		0	0	0
		2	0.708333	1	0	1	1	1	0	0	NA	NA		0	1	0
	2004	1	0.458333	0	0	0	0	0	0	0	NA	NA		0	0	0
		2	0.708333	1	0	1	1	1	0	0	NA	NA		0	1	0
E-1	2002	1	0.264286	0	0	0	0	0	0	0	NA	NA		0	0	0
		2	0.757143	0	0	0	0	0	0	0	NA	NA		0	0	0
	2003	1	0.307143	1	0	1	1	1	0	0	NA	NA		0	1	0
		2	0.821429	0	0	0	0	0	0	0	NA	NA		0	0	0
	2004	1	0.321429	3	0	1	3	0.6	0	0	NA	NA		1	2	0
		2	0.821429	0	0	0	0	0	0	0	NA	NA		0	0	0

[a]Disease incidence = Quadrat disease incidence.
[b]Number of [X,Y] lags significantly greater (SL+), or less (SL-) than expected by chance at $\alpha = 0.05$ level.
[c]Strength of aggregation = number of SL+ in core cluster / total number of SL+.
[d]Core cluster size = the number of significant SL+ lags contiguous with the [0,0]lag position that form a discrete group.
[e]Core Cluster Saturation = the 'proportion' of SL+ lags contiguous with the [0,0]lag position that form a discrete group bounded by the outermost lag extents.
[f]Reflected cluster size = the number of contiguous SL+ in various clusters not contiguous with the core cluster.
[g]Total number of clusters = the number of contiguous clusters of SL+ in the proximity pattern.
[h]Calculation of distance from centroid of core cluster to centroid of reflected cluster in x and y distance given in tree spaces and Calculated distance in meters.
[i]Effects = the number of SL+ within-row and within-column of the row and column defined by the [0,0] lag. Edge effects are significant (S) or non significant (ns) if (the number of SL+ at the distal edges of the proximity pattern / total number of SL+) is ≥5%, and <5%, respectively.

TABLE 3 (CONTINUED)
SPATIAL AUTOCORRELATION ANALYSIS OF FOUR PSOROSIS-AFFECTED CITRUS BLOCKS IN SOUTH TEXAS

Plot	Year	Scenario	Disease incidence[a]	Significant lags[b]		Strength of aggregation[c]	Core cluster size[d]	Core cluster saturation[e]	Reflected cluster size[f]	Total no. of reflected clusters[g]	SL+ reflected clusters[h]			Effects[i]		
				SL+	SL-						Max. X dist.	Max. Y dist.	Calc dist. (m)	Within row	Across row	Edge
F-1	2002	1	0.152778	3	0	0	0	NA	1	3	2	2	16.4	1	1	0
		2	0.833333	0	0	0	0	0	0	0	NA	NA		0	0	0
	2003	1	0.201389	6	0	0	0	NA	4,2	2	1.5	2	13.2	1	2	0
		2	0.833333	0	0	0	0	0	0	0	NA	NA		0	0	0
	2004	1	0.201389	6	0	0	0	NA	4,2	2	1.5	2	13.2	1	2	0
		2	0.833333	0	0	0	0	0	0	0	NA	NA		0	0	0

[a]Disease incidence = Quadrat disease incidence.
[b]Number of [X,Y] lags significantly greater (SL+), or less (SL-) than expected by chance at $\alpha = 0.05$ level.
[c]Strength of aggregation = number of SL+ in core cluster / total number of SL+.
[d]Core cluster size = the number of significant SL+ lags contiguous with the [0,0]lag position that form a discrete group.
[e]Core Cluster Saturation = the 'proportion' of SL+ lags contiguous with the [0,0]lag position that form a discrete group bounded by the outermost lag extents.
[f]Reflected cluster size = the number of contiguous SL+ in various clusters not contiguous with the core cluster.
[g]Total number of clusters = the number of contiguous clusters of SL+ in the proximity pattern.
[h]Calculation of distance from centroid of core cluster to centroid of reflected cluster in x and y distance given in tree spaces and Calculated distance in meters.
[i]Effects = the number of SL+ within-row and within-column of the row and column defined by the [0,0] lag. Edge effects are significant (S) or non significant (ns) if (the number of SL+ at the distal edges of the proximity pattern / total number of SL+) is ≥5%, and <5%, respectively.

be any appreciable difference in the two scenarios which treat the lowest rating of disease as either an indicator of disease or not.

If we consider all three levels of spatial hierarchy examined, we would conclude that psorosis exhibits a weak aggregation within a local area of influence, but that these groups of infected trees seem to be related over distance. Thus, there are weak indications that psorosis is acting as a contagion. Associations among symptomatic trees over longer distances were also indicated to some extent, which could imply the presence of a vector, however an inefficient one, if compared to other vectored pathogens of citrus.

Spatio-temporal stochastic model. In the present study we examined the spatio-temporal dynamics of psorosis in four plots using two different scenarios described above. However, unlike the analyses for aggregation at three hierarchical levels where interpretation of the analyses resulted in very similar conclusions concerning aggregation of spatial patterns regardless of scenario, when we examine the spatio-temporal dynamics of the spatial patterns through time, the differences between the two scenarios were quite pronounced. The difference is that for Scenario 1 a very slight amount of bark peeling and gumming was not considered necessarily indicative of psorosis, where these same indicators were considered as indicative of the virus infection for Scenario 2. Thus Scenario 2 considered more plants were infected with psorosis during each assessment date and thus a higher incidence of virus infection. The posterior density contours associated with the four plots for the psorosis pathosystem fell into two general cases and these did not align completely with the two scenarios based on symptoms.

Case 1: Two of the eight posterior density contour maps corresponded to cases where the a_2 was positioned towards the maximum of its range with the highest probability of ≥2.5 and b was clearly nonzero, usually in the range [0.5, 1.5] but with the highest probability of ≅1.0 (Fig. 2 A, D). A third contour map was related (Fig. 2H), however for this plot/scenario combination, a_2 was also positioned towards the maximum of its range (highest probability estimated to be ≥2.5). However, b had the highest probability of ≅0.5 but these was also some probability that b could also equal 0.

Case 2: In contrast, further inspection of the analogous posterior density maps indicated a second case and revealed a different situation (Fig. 2E). Here the estimated probability resided in a region of parameter space in which b is ≥0 but less than 1.0 and a_2 assumes values towards the lower end of its range, ≥0.5 to 2.1 with a maximum probability of ≅1.0. If we focus on only the highest likelihood region, we see that Figs. 2C and 2B have some similarity but if all including lower probability estimations are taken into account, we see that both a_2 and b can potentially span the entire range of values and therefore cannot be meaningfully interpreted for both surfaces. Finally for the two posterior density maps not here to for mentioned, the estimated range or probabilities spanned much of the total parameter density space, and are therefore both difficult to interpret and do not provided additional biological interpretation (Fig. 2F, G). Thus we must limit our interpretation to only four of the eight surfaces (Fig. 2A, D, E, H).

Interpretation of these two cases of the spatio-temporal stochastic model results leads to differing conclusions concerning psorosis spread. For case 1, the model suggested that psorosis spread through a combination of random background transmission and a local transmission that operated over short distances and was predominately nearest neighbor and was the predominate situation for three of the four plots studies. If we consider that the background

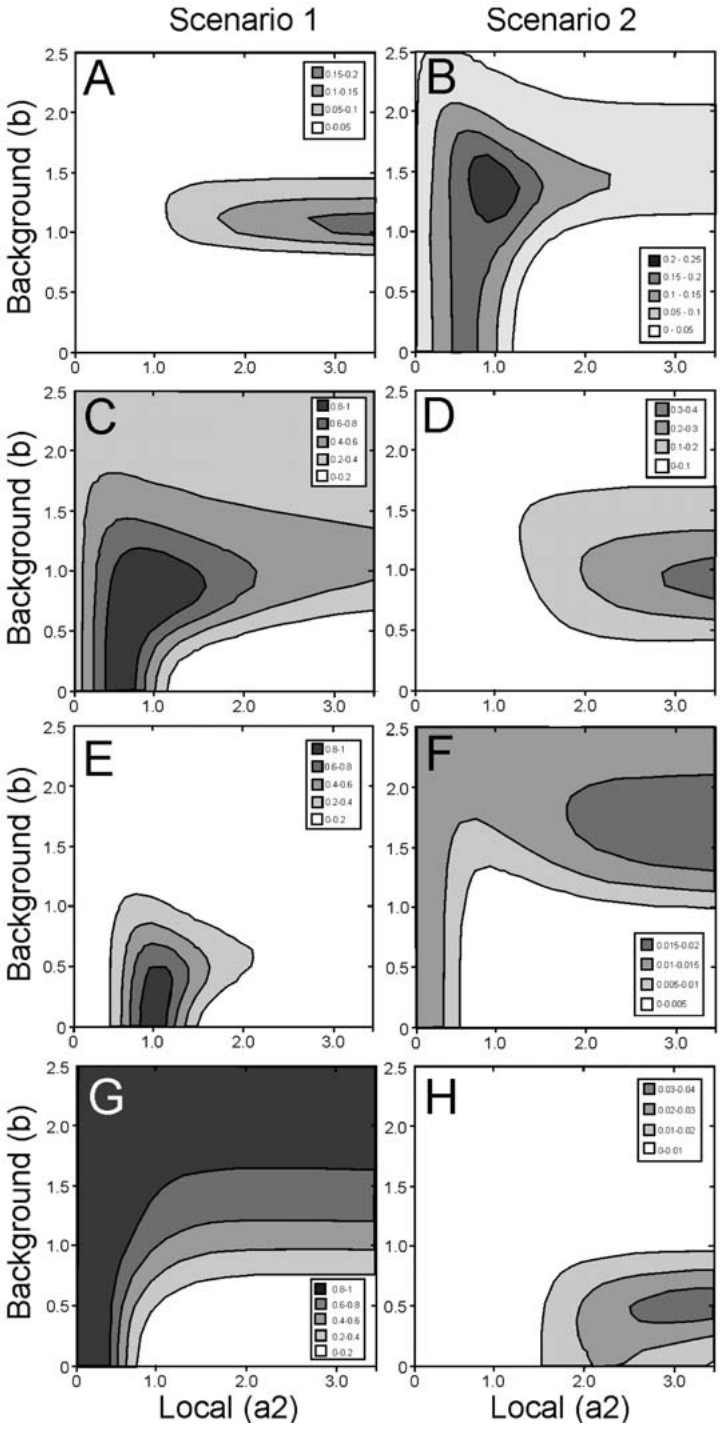

Fig. 2. Posterior density estimates of Markov-Chain Monte Carlo Simulation of the Spatio-temporal increase of psorosis in citrus plots in south Texas. MCMC posterior density likelihood estimations for local and background influences on disease spread for A,B) Plot A4; C, D) Plot B5; E, F) Plot E1, and Plot F1 (G, H), for Scenarios 1 and 2, respectively. Contour maps represent posterior density estimations $L(a)$ composited over all assessments for the duration of the study for each plot with a minimum of 5% increase in disease incidence between individual assessments.

transmission or primary infection is the result of inoculum sources outside the plots, then this is similar to the spatio-temporal stochastic model results for *Citrus tristeza virus* (CTV) with vectors predominately of the migratory type (9). However, we must also consider that if psorosis is soilborne *via* some mechanism or vector, then we cannot discard the possibility of resident inoculum that is contributing apparently random infections within the plot.

In contrast, for case 2 the results suggested a short-range local infection mechanism which was not restricted to nearest-neighbor interactions. Results also suggested that transmission may have been purely local and that the presence of background infection from sources outside the plot or from soilborne sources was not necessary to explain the observed virus spread. This is similar to the model results for CTV with vectors predominately of the colonizing type (9).

Of course, other interpretations such as a complete lack of a vector are possible. However, if an *Olpidium*-like fungus is associated with the roots of psorosis-infected trees, and the virus can be spread in zoospores, then the two possible cases of virus spread discussed above need to be examined from this perspective. Certainly nearest neighbor and tree to adjacent tree transmission would make sense as virus-infected zoospores could move in irrigation or rain water from tree to tree and even several trees around if some ground flooding occurs. However, transmission across multiple rows especially at oblique angles and over longer distances suggest that other spatial mechanisms in addition to surface water movement would have to come into play. Mechanical spread of zoospore-infected soil and/or zoospore-laden water is one possibility and many chances exist for such an occurrence. The orchards studied were flood irrigated, and banks were made approximately every third row. This means that there is a potential for some soil to be moved each time during irrigation, and that there is some lateral spread of water across rows. We must also consider that at times there was indication of background or primary infection that was not distinguishable for a random resident source of inoculum. During various orchard management practices such as spraying, harvesting, etc., there is potential for mechanical movement of soil on tires, boots, etc. which could deposit isolated new sources of soilborne inoculum. In addition, we also cannot eliminate the possibility of an aerial vector also playing a role as suggested by others (1, 22), nor the possibility that some trees are affected by non-psorosis bark scaling, especially considering that one symptomatic tree did not test positive by ELISA or PCR. Therefore from a spatio-temporal context, for the spread of psorosis in the plots studied the interpretation is unclear, with possible multiple interpretations including aerial and/or soilborne vectors that could contribute to both local and longer distance dispersal of disease.

ACKNOWLEDGMENTS

The authors wish to thank Jolene Taylor for efforts in conducting numerous statistical procedures.

LITERATURE CITED

1. Beñatena, H. N. and M. M. Portillo
1984. Natural spread of psorosis in sweet orange seedlings. In: *Proc. 9th Conf. IOCV,* 159-164. IOCV, Riverside CA.
2. Campbell, C. L. and L. V. Madden
1990. *Introduction to Plant Disease Epidemiology.* John Wiley & Sons, New York.
3. Fawcett, H. S.
1948. Psorosis (scaly bark) in the Rio Grande Valley. Texas Fmg. & Citricult. 25(1): 6; (2): 8; (3): 15-16.

4. Gibson, G. J.
1997. Investigating mechanisms of spatiotemporal epidemic spread using stochastic models. Phytopathology 87: 139-146.
5. Gibson, G. J.
1997. Markov chain Monte Carlo methods for fitting spatiotemporal epidemic stochastic models in plant pathology. Appl. Stat. 46: 215-233.
6. Gibson, G. J.
1997. Fitting and testing spatiotemporal stochastic models with applications in plant pathology. Plant Pathol. 45: 172-184.
7. Gottwald, T. R., S. M. Richie, and C. L. Campbell
1992. LCOR2-spatial correlation analysis software for the personal computer. Plant Dis. 76: 213-215.
8. Gottwald, T. R., S. M. Garnsey, and J. Borbón
1998. Increase and patterns of spread of citrus tristeza virus infections in Costa Rica and the Dominican Republic in the presence of the brown citrus aphid, *Toxoptera citricida*. Phytopathology 88: 621-636.
9. Gottwald, T. R., G. Gibson, S. M. Garnsey, and M. Irey
1999. Examination of the effect of aphid vector population composition on the spatial dynamics of citrus tristeza virus spread via stochastic modeling. Phytopathology 89: 603-608.
10. Hughes, G. and L. V. Madden
1993. Using the beta-binomial distribution to describe aggregated patterns of disease incidence. Phytopathology 83: 759-763.
11. Lot, H., R. N. Campbell, S. Couche, R. G. Milne and P. Roggero
2002. Transmisison by *Olpidium brassicae* of *Mirafiori lettuce virus* and *Lettuce big-vein virus* and their roles in lettuce big-vein etiology. Phytopathology 92: 288-293
12. Madden, L. V. and G. Hughes
1994. BBD-Computer software for fitting the beta-binomial distribution to disease incidence data. Plant Dis. 78: 536-540.
13. Madden, L. V. and G. Hughes
1995. Plant disease incidence: distributions, heterogeneity, and temporal analysis. Annu. Rev. Phytopathol. 33: 529-564.
14. Madden, L. V., R. Louie, J. J. Abt, and J. K. Knoke
1982. Evaluation of tests for randomness of infected plants. Phytopathology 72: 195-198.
15. Madden, L. V., L. R. Nault, D. J. Murral, and M. R. Apelt
1995. Spatial pattern analysis of the incidence of Aster Yellows disease in lettuce. Res. Popul. Ecol. 37: 279-289.
16. Martín, S., R. G. Milne, D. Alioto, J. Guerri, and P. Moreno
2002. Psorosis-like symptoms induced by causes other than *Citrus psorosis virus*. In: *Proc. 15th Conf. IOCV*, 197-204. IOCV, Riverside, CA.
17. Martín, S., D. Alioto, R. G. Milne, S. M. Garnsey, M. L. García, O. Grau, J. Guerri, and P. Moreno
2004. Detection of *Citrus psorosis virus* by ELISA, molecular hybridization, TR-PCR and immunosorbent electron microscopy and its association with citrus psorosis disease. Eur. J. Plant Pathol. 110: 747-757.
18. Palle, S. R., H. Miao, M. Seyran, E. S. Louzada, J. V. da Graça, and M. Skaria
2005. Evidence for association of *Citrus psorosis virus* with symptomatic trees and an *Olpidium*-like fungus. In: *Proc. 16th Conf. IOCV*, 423-426. IOCV, Riverside CA.
19. Skaria, M.
2004. People, arthropods, weather and citrus diseases. *Diseases of Fruits and Vegetables Vol. I,* S.A.M.H.Naqvi (ed.), 307-337. Kluwer Press, Dordrecht.
20. Skaria, M., H. Miao and E. Avila
2002. Post-freeze status of citrus psorosis virus in Texas. In: *Proc. 15th Conf. IOCV,* 366-367. IOCV, Riverside, CA.
21. Sleeth, B.
1959. The citrus budwood certification program in Texas. *Citrus Virus Diseases*, J. M. Wallace (ed.), 233-236. Univ. Calif. Press, Riverside.
22. Timmer, L. W. and S. M. Garnsey
1980. Natural spread of citrus ringspot virus in Texas and its association with possible diseases in Florida and Texas. In: *Proc. 8th Conf. IOCV,* 167-173. IOCV, Riverside, CA.
23. Upton, G., and B. Fingleton
1985. *Spatial Data Analysis by Example. Vol. 1: Point Pattern and Quantitative Data*. John Wiley & Sons, Chichester.
24. Wallace, J. M.
1978. Virus and virus-like diseases. *The Citrus Industry Vol. 4*, W. Reuther, E. C. Calavan, and G. E. Carman (eds.), 67-184. Univ. California Div. Agric. Sci.